RSC

New Journal of Chemistry (NJC)

Supporting information

Enhancing carminic acid anticancer potential: transforming a conventional nanocarrier to a multifunctional therapeutic nanoplatform for photodynamic ROS generation and FRET-based tracking

Fatemeh Bahadorani [a], Hassan Hadadzadeh [a,*], Seyede Zohreh Mirahmadi-Zare [b,*], Hossein Farrokhpour [a], Zahra Amirghofran [c], Marziyeh Poshteh Shirani [a]

[a] Department of Chemistry, Isfahan University of Technology, Isfahan 84156-83111, Iran

[b] Department of Animal Biotechnology, Reproductive Biomedicine Research Center, Royan Institute for Biotechnology, ACECR, 8159358686, Isfahan, Iran

[c] Immunology Department and Autoimmune Diseases Research Center, Shiraz University of Medical Sciences, Shiraz, Iran

[*] Corresponding authors:

Hassan Hadadzadeh, Professor of Inorganic and Bioinorganic Chemistry, Department of Chemistry, Isfahan University of Technology, Isfahan 84156-83111, Iran; E-mail address: hadad@iut.ac.ir

Seyede Zohreh Mirahmadi-Zare, Associate Professor of Analytical Chemistry, Department of Animal Biotechnology, Reproductive Biomedicine Research Center, Royan Institute for Biotechnology, ACECR, Isfahan 81651-31378, Iran; E-mail address: mirahmadi_zare@royaninstitute.org

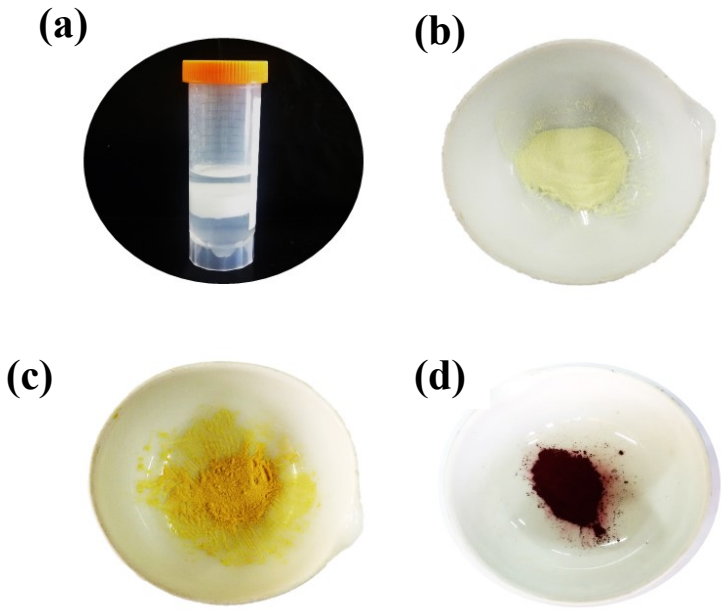

Figure S1. Physical view of the synthesized nanoparticles (a) hydrogel of MSNs, (b) NH_2-MSNs, (c) FA-MSNs, and (d) CA@FA-MSNs.

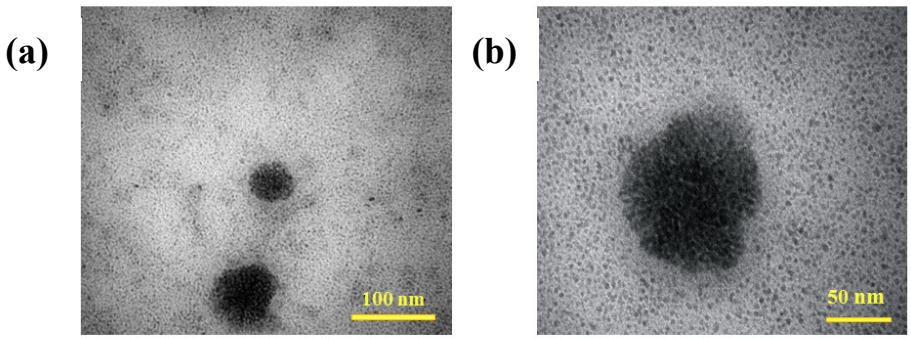

Figure S2. TEM images of FA-MSNs.

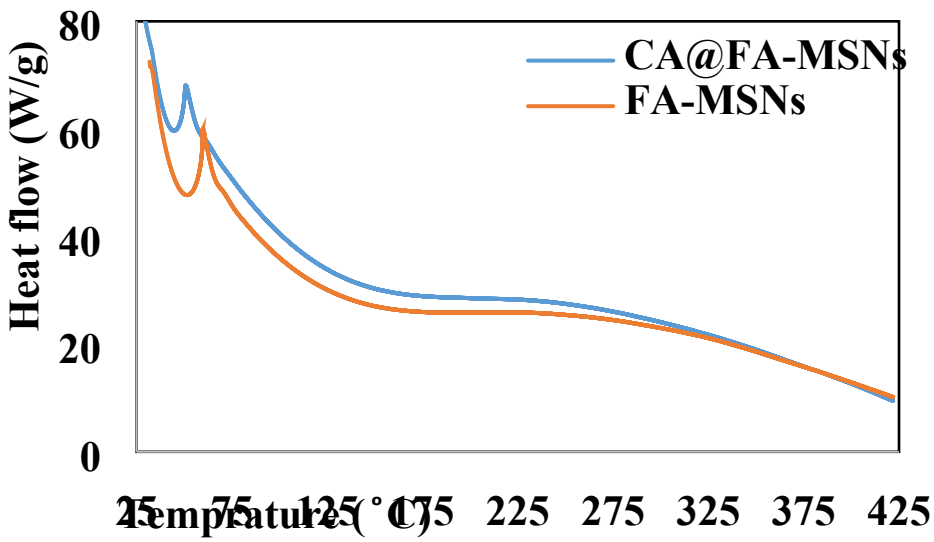

Figure S3. DSC of FA-MSNs and CA@FA-MSNs.

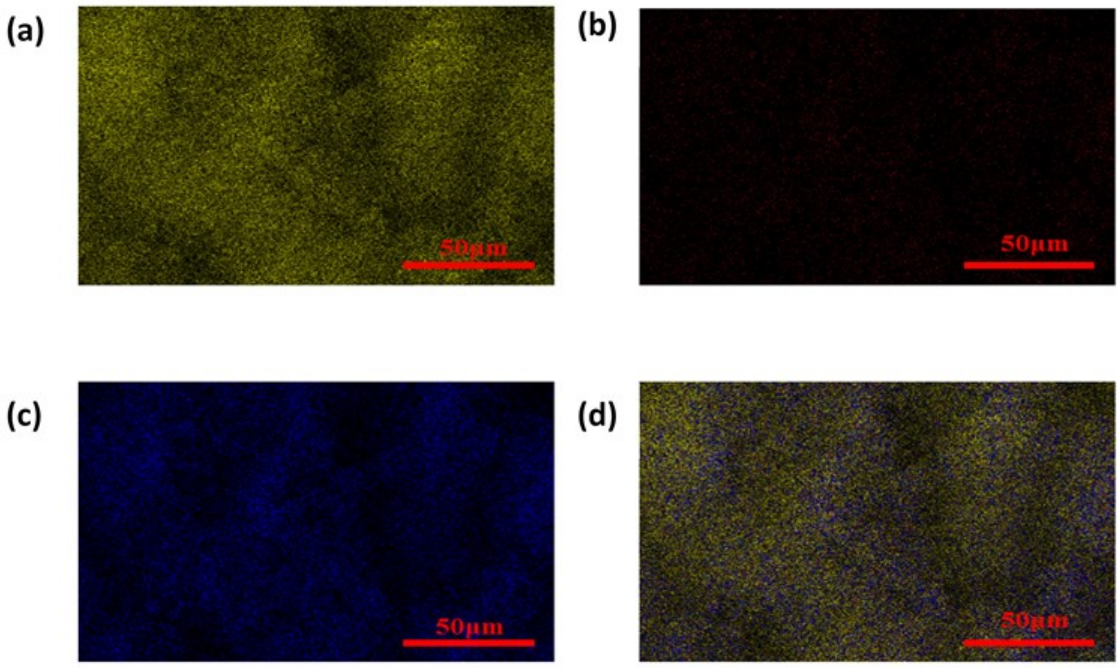

Figure S4. EDS mapping of MSNs. (a) Si atoms, (b) C atoms, (c) O atoms, and (d) distribution of atoms.

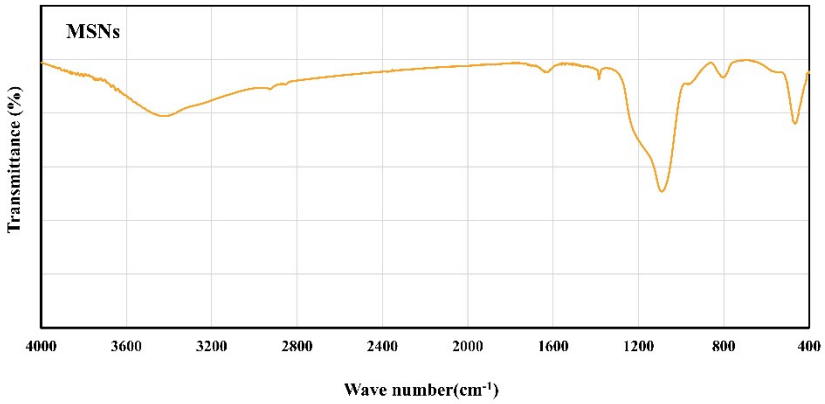

Figure S5. FT-IR spectrum of MSNs after calcination.

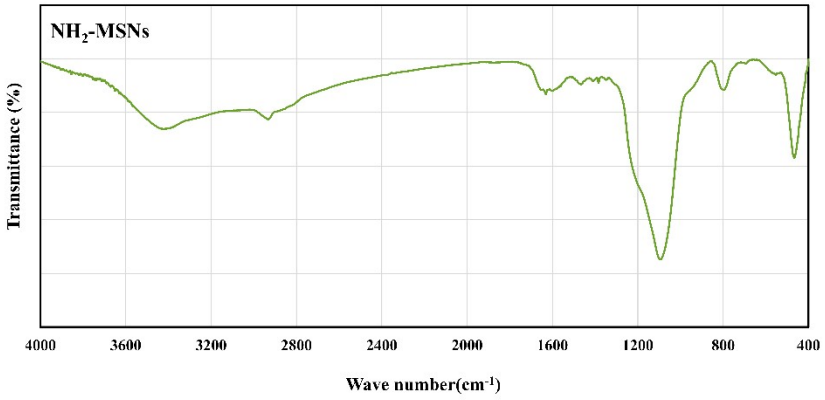

Figure S6. FT-IR spectrum of NH_2-MSNs.

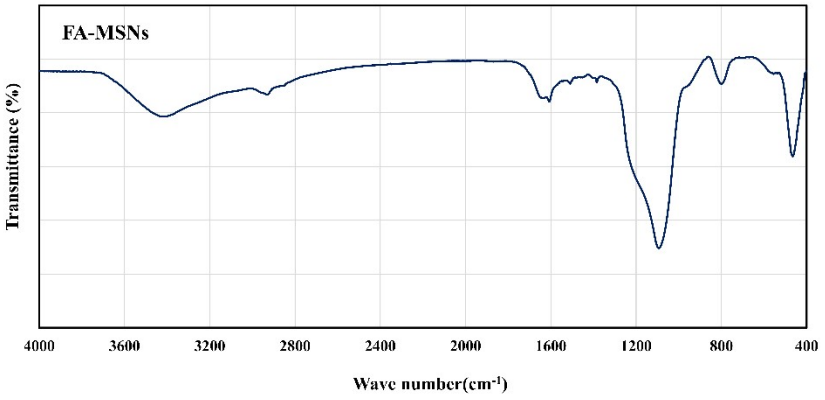

Figure S7. FT-IR spectrum of FA-MSNs.

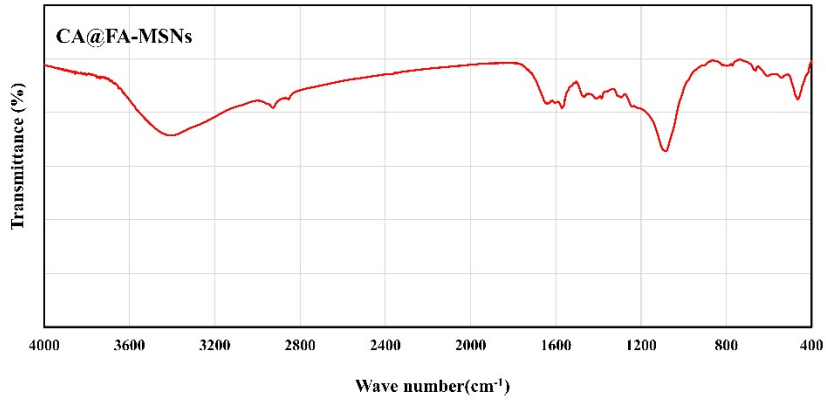

Figure S8. FT-IR spectrum of CA@FA-MSNs.

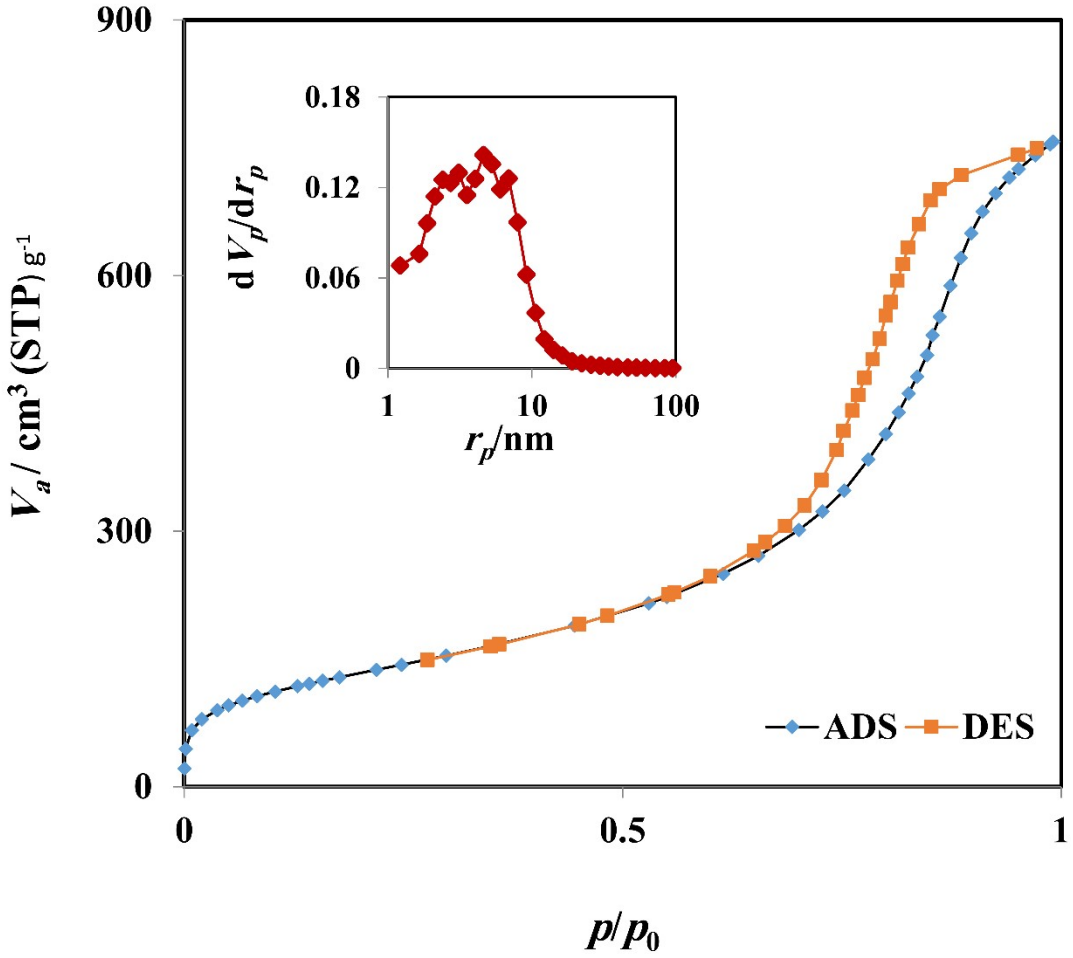

Figure S9. BET and BJH data of MSNs.

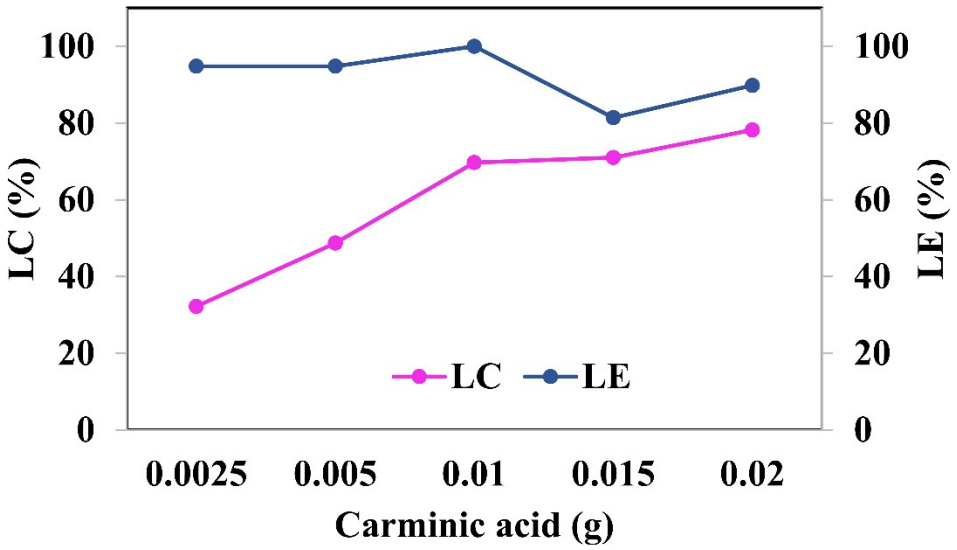

Figure S10. LC and LE of FA-MSNs.

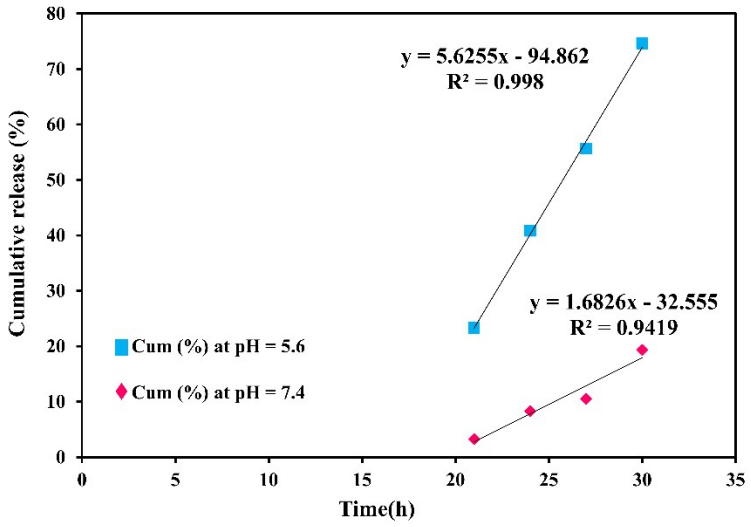

Figure S11. Zero-order plot of the CA@FA-MSNs release.

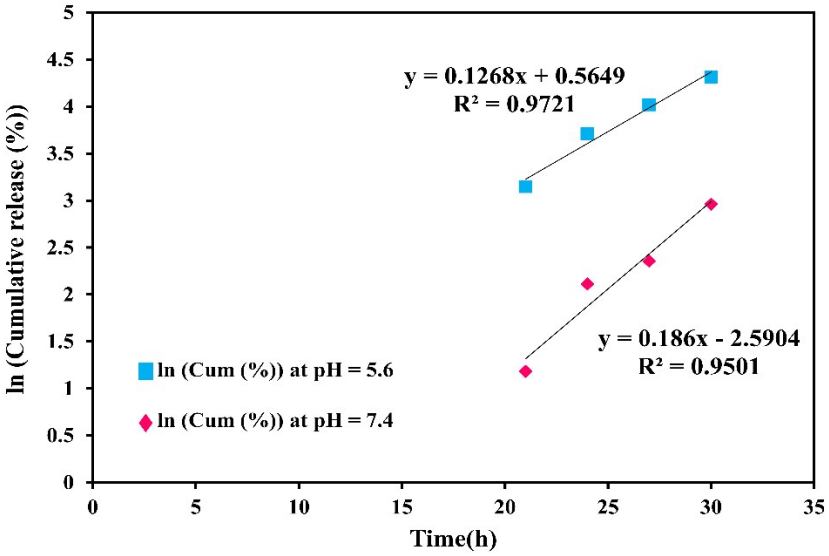

Figure S12. First-order plot of the CA@FA-MSNs release.

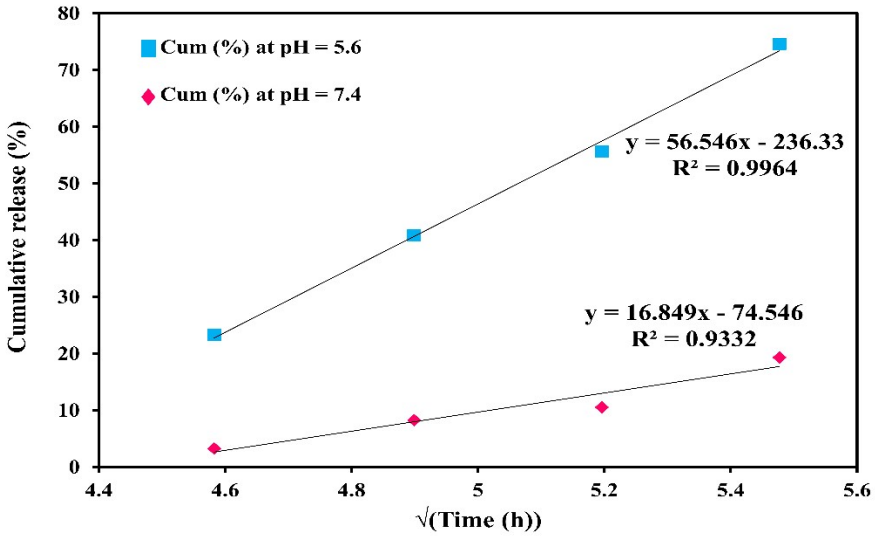

Figure S13. Higuchi's plot of the CA@FA-MSNs release.

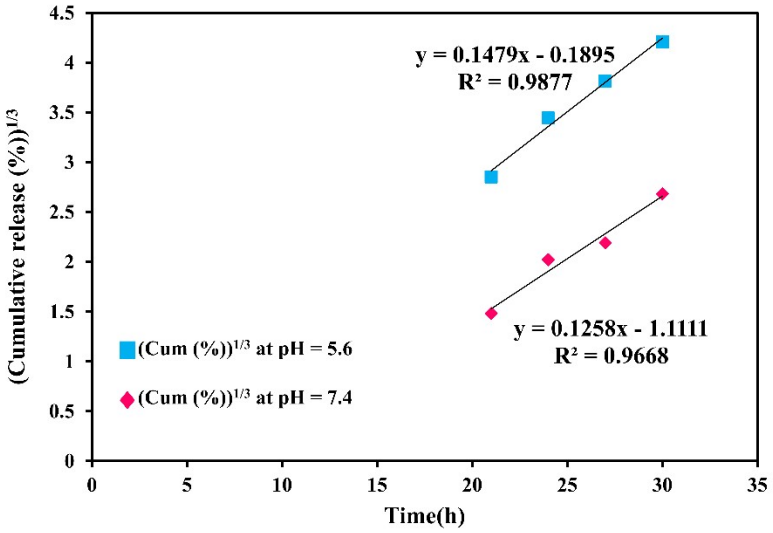

Figure S14. Hixson-Crowell's plot of the CA@FA-MSNs release.

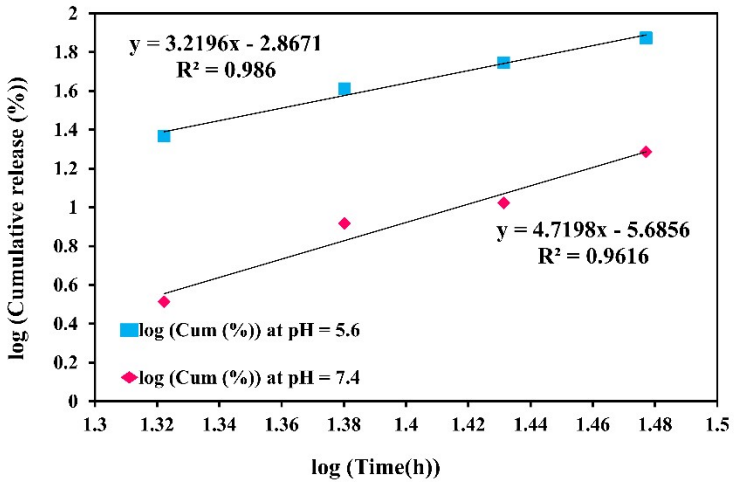

Figure S15. Korsmeyer-Peppa's plot of the CA@FA-MSNs release.

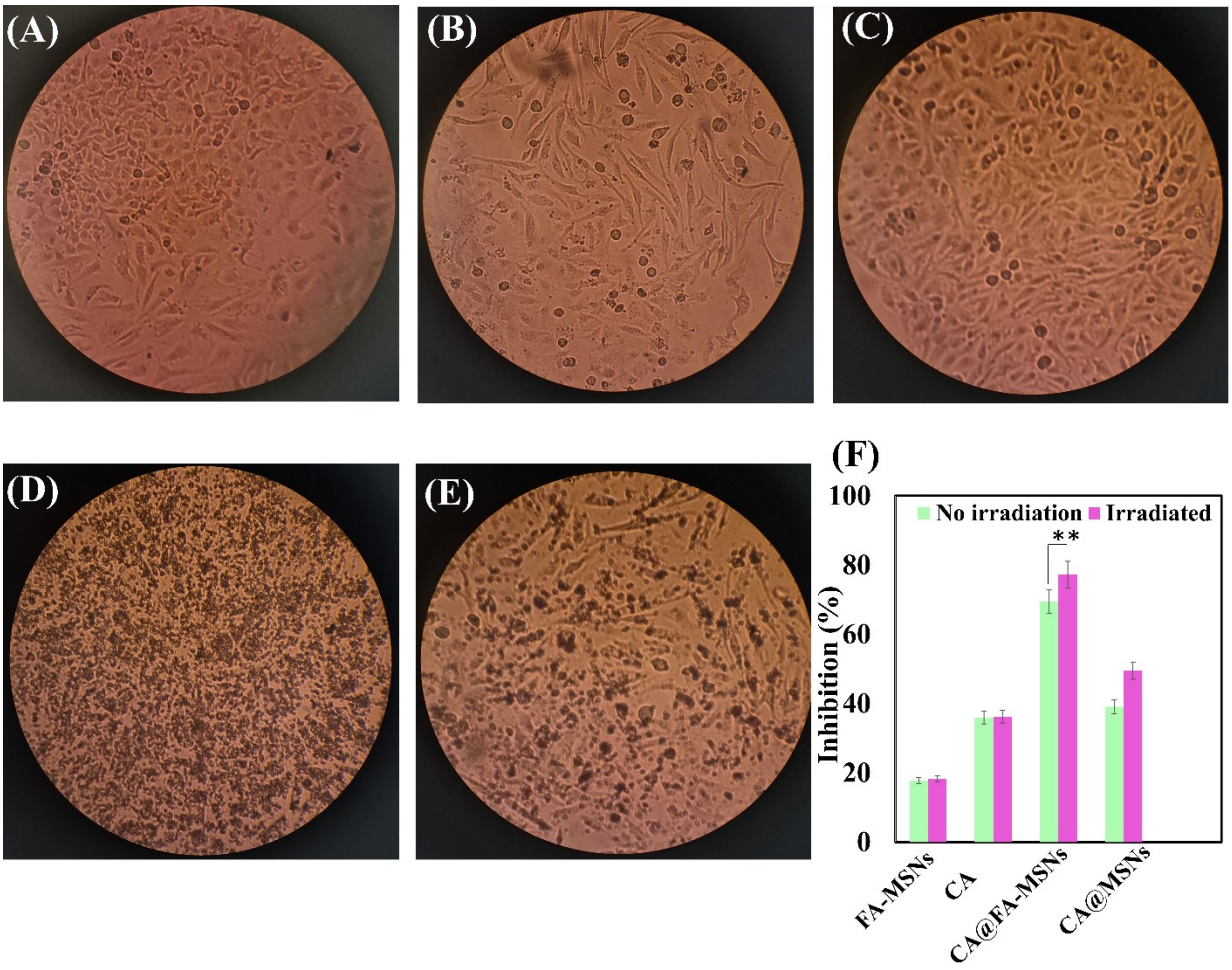

Figure S16. Optical microscopic image of HeLa cells treating with 100 µg/mL of (A) control, (B) FA-MSNs, (C) CA, (D) CA@FAMSNs, and (E) CA@MSNs after UVB irradiation; (F) the comparison between cytotoxicity of FA-MSNs, CA, CA@FA-MSNs, and CA@MSNs in irradiated and non-irradiated groups.

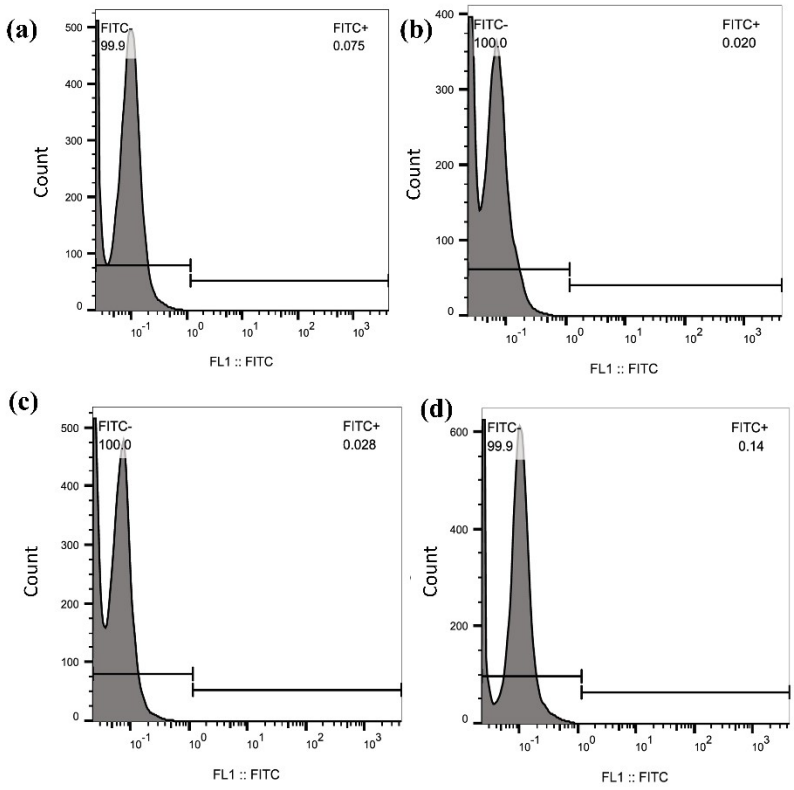

Figure S17. Flow cytometry results in FL1, (a) CA, (b) CA@FA-MSNs, (c) CA@MSNs, and (d) unstained.

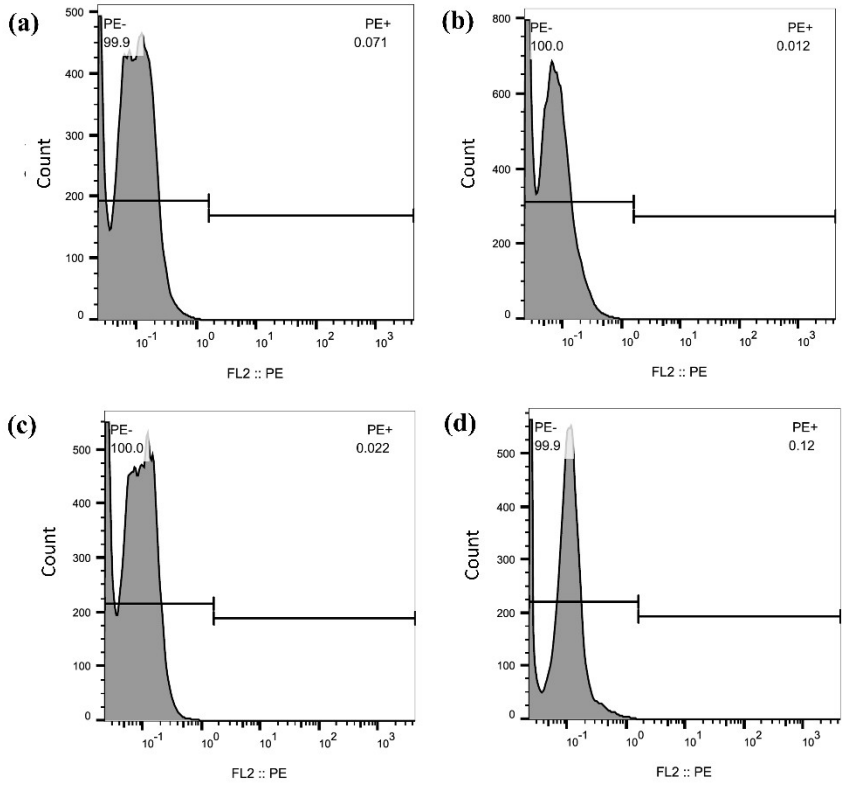

Figure S18. Flow cytometry results in FL2, (a) CA, (b) CA@FA-MSNs, (c) CA@MSNs, and (d) unstained.

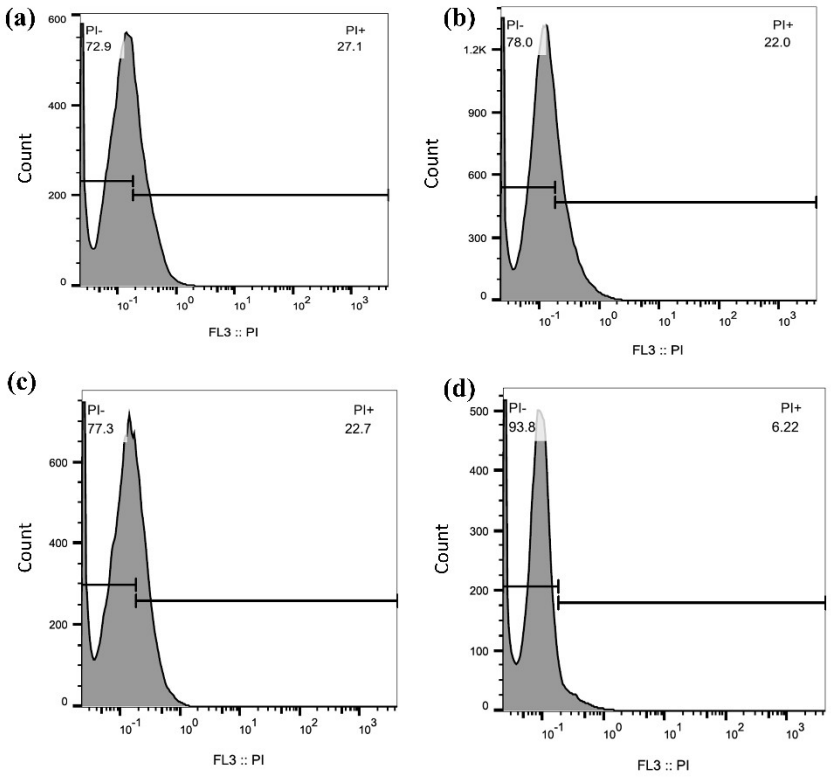

Figure S19. Flow cytometry results in FL3, (a) CA, (b) CA@FA-MSNs, (c) CA@MSNs, and (d) unstained.

.